Magn Reson Med Sci 2021; 20; 227–230
doi:10.2463/mrms.bc.2020-0046
Published Online: July 1, 2020

BRIEF COMMUNICATION

Time-dependent Diffusion in Transient Splenial Lesion: Comparison between Oscillating-gradient Spin-echo Measurements and Monte-Carlo Simulation

Tomoko Maekawa[1,2], Kouhei Kamiya[1,2,5*], Katsutoshi Murata[3], Thorsten Feiweier[4], Masaaki Hori[1,5], and Shigeki Aoki[1]

The microstructural underpinnings of reduced diffusivity in transient splenial lesion remain unclear. Here, we report findings from oscillating gradient spin-echo (OGSE) diffusion imaging in a case of transient splenial lesion. Compared with normal-appearing white matter, the splenial lesion exhibited greater differences between diffusion time t = 6.5 and 35.2 ms, indicating microstructural changes occurring within the corresponding length scale. We also conducted 2D Monte-Carlo simulation. The results suggested that emergence of small and non-exchanging compartment, as often imagined in intramyelinic edema, does not fit well with the *in vivo* observation. Simulations with axonal swelling and microglial infiltration yielded results closer to the *in vivo* observations. The present report exemplifies the importance of controlling t for more specific radiological image interpretations.

Keywords: *diffusion time, microstructure, OGSE, simulation, transient splenial lesion*

The pathophysiology of the transient splenial lesion, a reversible focal reduction of apparent diffusion coefficient (ADC) in the splenium of the corpus callosum, remains obscure, despite the widespread recognition of this phenomenon. Transient splenial lesions occur during various clinical conditions, including infection, withdrawal of antiepileptic drugs, drug toxicity, hypoglycemia, malnutrition, high-altitude disease, and Charcot–Marie–Tooth disease.[1] This lesion usually resolves quickly without neurological sequelae, implying a distinct pathology from ischemic infarction, though the lesion exhibits ADC values comparable to that of infarction.

An emerging field of diffusion MRI (dMRI) is to probe tissue microstructure by varying the diffusion time.[2] Due to the presence of obstacles (e.g., cell membranes, organelles, myelin, extracellular structures), dMRI measurements in biological tissues are dependent on the effective diffusion time (t), the time interval over which spin displacements are sampled. Time-dependent diffusion has been observed in both healthy[3,4] and diseased[5–7] human organs. These observations are important for clinical practice, because they mean that radiological image interpretation can be improved by controlling t. Selecting a dedicated t that maximizes the contrast between lesions and normal tissue will improve sensitivity. In addition, studying diffusivity as a function of diffusion time, $D(t)$, enables characterization of microstructural features. For example, the lesion contrast for acute infarction diminished in a shorter t realized by oscillating gradient spin-echo (OGSE) compared with a longer t by conventional pulsed gradient spin-echo (PGSE) diffusion imaging.[5] Based on the form of $D(t)$, it has been suggested that the reduction of diffusivity in acute infarction can be well explained by neurite beading.[2,5] Here, we report a case of transient splenial lesion with findings on OGSE, along with hypothesizing regarding the underlying microstructure based on simple computer simulation.

A 49 year-old male presented with fever and inarticulate speech lasting for 6 days. After physical examination and laboratory tests, he was referred for brain MRI as part of the diagnostic work-up for viral meningitis. MRI on the 3T scanner (MAGNETOM Prisma, Siemens Healthcare, Erlangen, Germany) revealed characteristic oval hyperintensity in the splenium on diffusion-weighted image (DWI) with PGSE. The OGSE protocol used a trapezoid-cosine waveform with a frequency of 30 Hz; all other parameters were identical between PGSE and OGSE: TR, 4800 ms; TE, 101 ms; voxel size, 2.5 × 2.5 × 5 mm^3; 30 axial slices; and scan time, approximately 2 min. Both OGSE and PGSE used b = 1000 s/mm^2 with six diffusion-encoding directions. The effective diffusion time for

[1]Department of Radiology, Juntendo University School of Medicine, Tokyo, Japan
[2]Department of Radiology, The University of Tokyo, Tokyo, Japan
[3]Siemens Healthcare K.K., Tokyo, Japan
[4]Siemens Healthcare GmbH, Erlangen, Germany
[5]Department of Radiology, Toho University, Tokyo, Japan

*Corresponding author: Department of Radiology, The University of Tokyo, 7-3-1, Hongo, Bunkyo-ku, Tokyo 113-8655, Japan. Phone: +81-3-5800-8666, Fax: +81-3-5800-8935, E-mail: kkamiya-tky@umin.ac.jp

Received: March 17, 2020 | Accepted: April 24, 2020

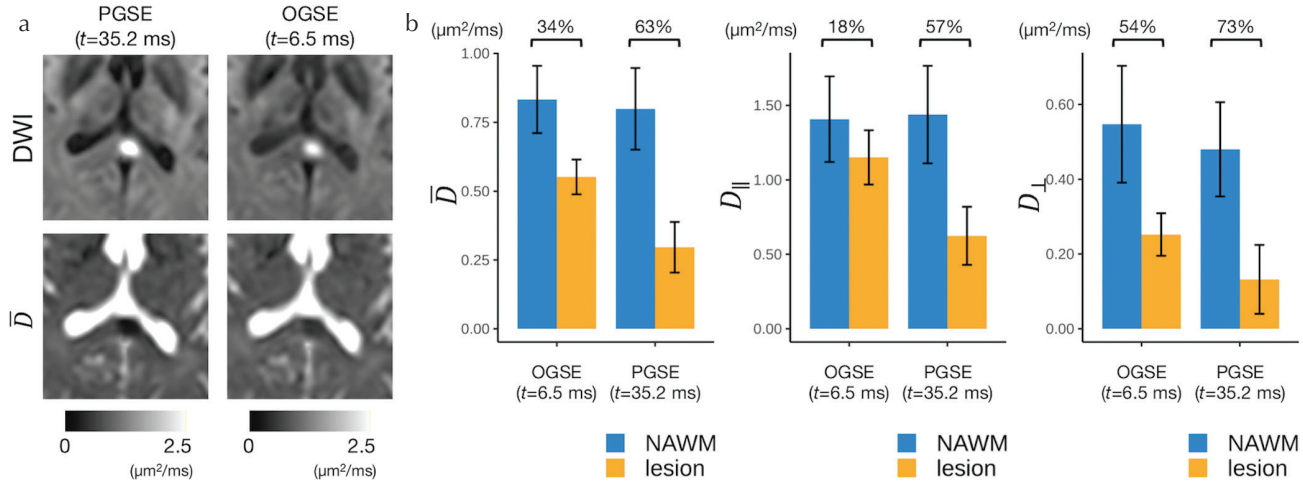

Fig. 1 (a) DWIs (top) and D maps (bottom) for PGSE (left) and OGSE (right). (b) Measured diffusivities (mean ± 1 SD) in the splenial lesion and NAWM. Above the bar chart are the relative ratios of diffusivity reduction $[(D_{NAWM} - D_{lesion})/D_{NAWM}]$. The lesion exhibited reduced diffusivity on both OGSE and PGSE. The reduction was weaker in OGSE. DWIs, diffusion-weighted images; NAWM, normal-appearing white matter; OGSE, oscillating gradient spin-echo; PGSE, pulsed gradient spin-echo.

OGSE, calculated as in Baron et al.,[3] was $t = 6.5$ ms; for PGSE, it was $t = 35.2$ ms ($\Delta - \frac{\delta}{3}$, $\Delta = 47.3$ ms and $\delta = 36.3$ ms). Note that the definitions of t for both OGSE and PGSE are not universal but dependent on the functional form of $D(t)$ and thus still a matter of debate.[2] Here, we selected the commonly used definitions[3] for comparison with the literature.

Figure 1 shows the DWIs and diffusivity values. The mean/parallel/perpendicular diffusivities ($\bar{D}/D_{\parallel}/D_{\perp}$) were computed through a standard diffusion tensor imaging procedure. The region of interest was placed manually to include the hyperintense area in DWI with PGSE. For reference, normal-appearing white matter (NAWM), presumably containing a population of single fibers, was defined by segmenting the $b = 0$ image using FMRIB's automated segmentation tool (FAST) in FMRIB software library (FSL) and further applying a threshold of fractional anisotropy ≥0.5. Compared with NAWM, the lesion exhibited decreased diffusivity on both OGSE and PGSE, although the reduction was weaker in OGSE (63%/34% [PGSE/OGSE] for $\bar{D}$, 57%/18% for $D_{\parallel}$, 73%/54% for $D_{\perp}$).

Hypothetical mechanisms of ADC reduction in transient splenial lesion include intramyelinic edema, inflammatory infiltrates, and axonal swelling.[1] With intramyelinic edema, splitting of myelin layers is thought to lead to an emergence of water molecules residing within small spaces between layers, which are strongly restricted in all directions. Intramyelinic edema has been observed histologically in several diseases with transient reduction of ADC, such as maple syrup urine disease.[8] Axonal swelling and inflammation-associated microglial infiltration are thought to increase the proportion of restricted intracellular compartments and to promote diffusion hindrance in the narrowed extra-cellular space. To gain insight into how intramyelinic edema, inflammatory infiltrates, and axonal swelling might each affect $D(t)$, we performed Monte-Carlo simulations, as outlined in a recent review.[9]

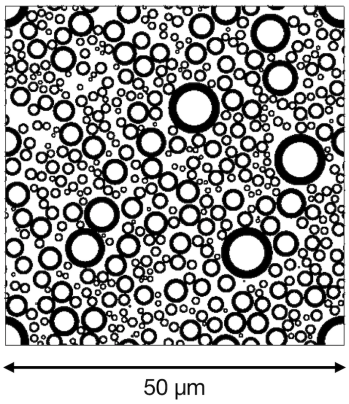

Fig. 2 Microgeometry used for the simulation (baseline state). Axons were modeled as randomly packed cylinders (circles). Signal contribution from myelin (black) was ignored due to its short T_2. For the baseline state, we used a uniform g-ratio of 0.7, and axonal fraction (including myelin) was set at 0.6. For all simulations, the field of view (50 × 50 μm²) and the number of axons in the field were held constant. We assumed intrinsic diffusivity as $D_0 \equiv D|_{t=0} = 2.0\ \mu m^2/ms$ for all compartments, uniform particle density and relaxation time, and negligible intercompartmental exchange. Each simulation is comprised of 5×10^4 particles and a time step of 5×10^{-5} ms. $D(t)$ was computed directly from particle displacement (i.e., diffusivities that would be observed with PGSE in a narrow pulse limit).

For simplicity, we used a two-dimensional model mimicking diffusion perpendicular to the axon, $D_{\perp}(t)$. Axons were modeled as randomly packed[10] cylinders (circles), with the inner diameters taken from a postmortem study[11] (Fig. 2). For axonal swelling, we increased the axonal inner diameters uniformly, while keeping the myelin volume constant. Microglias were modeled as circles (radius, 5 μm). Intramyelinic edema was represented as small circular holes (radius, 0.13–0.48 μm) within the myelin sheath.

Figure 3 shows the results of our simulations. In agreement with the *in vivo* results and previous works,[3,4] for the baseline

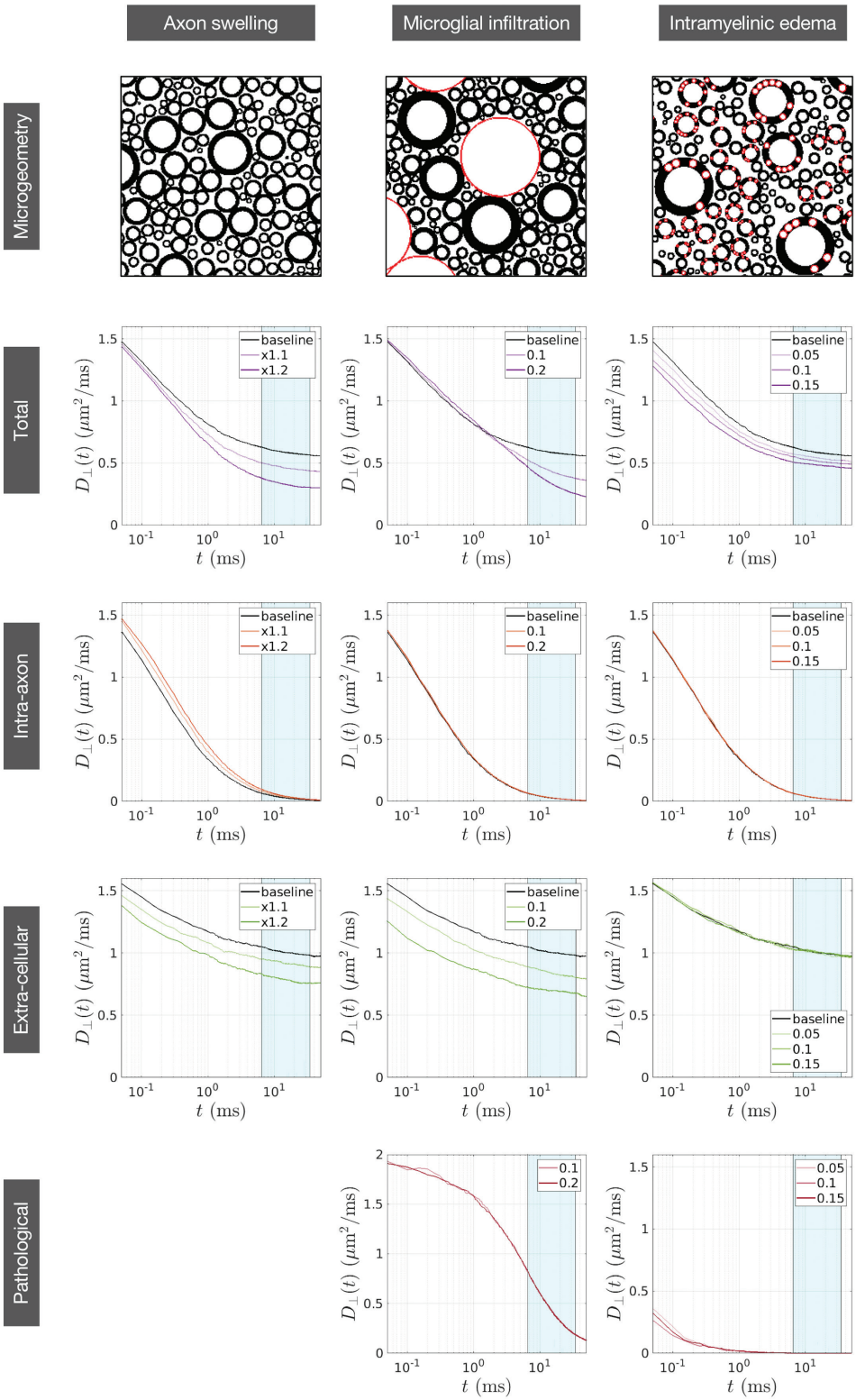

Fig. 3 The three pathological scenarios: axonal swelling (left), microglial infiltration (middle), and intramyelinic edema (right). The top row shows the microgeometries. For axonal swelling, the inner diameters of axons were increased by a factor of up to 1.2, while the myelin volume was kept constant. Microglias were modeled as circles (radius, 5 μm), and the fraction of microglias (red circles) was varied from 0 (baseline) to 0.2. Intramyelinic edema was modeled as small holes (radius, 0.13–0.48 μm) within the myelin sheath. The proportion of intramyelinic holes (red circles) was varied from 0 to 0.15. The second row shows the total diffusivities within a voxel; the bottom three rows show the diffusivity in each compartment [intra-axonal space, extracellular space, and pathological compartment (microglias or intramyelinic edema)]. The shaded area corresponds to the range of clinical data (t = 6.5–35.2 ms). Microglial infiltration led to greater difference from the baseline state at t = 35.2 ms than at t = 6.5 ms, in agreement with the *in vivo* observation. Similar trend was seen for axonal swelling, though the change between t = 6.5 and 35.2 ms was smaller. Intramyelinic edema did not alter the magnitude of difference from the baseline state between t = 6.5 and 35.2 ms.

state, total $D_\perp(t)$ exhibited small but meaningful differences in the range of t = 6.5–35.2 ms. Although all three of the pathological scenarios led to reduced total $D_\perp(t)$, intramyelinic edema did not yield an increase in the slope of $D_\perp(t)$ between t = 6.5–35.2 ms as observed *in vivo*. Whereas axonal swelling led to increased difference of diffusivities between t = 6.5–35.2 ms, as in Baron et al.,[5] microglial infiltration showed more pronounced effects, reflecting larger changes of length scales.

The present *in vivo* observation and computer simulation suggest that the emergence of water molecules confined inside very small subcellular structures, as often imagined in intramyelinic edema hypothesis, does not fit well with *in vivo* data, and the pathology responsible for transient splenial lesions has length scales which correspond to the diffusion distance explored by water molecules between t = 6.5 and 35.2 ms. Simulation with axonal swelling and microglial infiltration yielded trends similar to the *in vivo* observation, while the difference between t = 6.5 and 35.2 ms was smaller for axonal swelling. However, it is still too early to preclude intramyelinic edema as the mechanism for reduced ADC. Ignoring intercompartmental exchange was a crude assumption in our simulation, and introducing intercompartmental exchange into the simulation may possibly support intramyelinic edema. In addition, intramyelinic clefts may be much wider than our simulation (as seen in Fig. 4 in Harkins et al.[12]) such that intramyelinic edema was similar in effect to microglias in the present simulation.

The present simulation has lots of oversimplifications that need to be addressed in future. In reality, axonal swelling is non-uniform, and selective vulnerability of thin, un-myelinated axons is possible. Microglias are not spherical in shape but have complex geometries that change in response to inflammation. Though microglial infiltration yielded results closer to the *in vivo* data in the present simulation, incorporating permeability of microglia may lead to different conclusions. Our simulation also ignored the effects of shape variation of axons in the parallel direction (e.g., axonal beading) and orientation dispersion. Though our two-dimensional model represented both axons and microglias as circles, in three dimension, cylinders and spheres have different functional forms of $D(t)$.[9] Implementing all the geometric complexites (the distribution of axon radii, beading, dispersion, and dense packing, etc.) at the same time is extremely challenging, and we must wait for future developments of packing algorithms.

To summarize, the present findings suggest that the underlying pathology of transient splenial lesion has a structural length scale matching to the water molecule displacement during the range of diffusion times accessible with modern clinical scanners. Our report further supports that controlling t potentially enables more specific radiological image interpretation in future.

Acknowledgments

This study was supported in part by Japan Society for the Promotion of Science (JSPS) KAKENHI (grant numbers 18K07729 and 18K15643). We thank Hong-Hsi Lee, Dmitry S Novikov, Lauren M Burcaw, and Els Fieremans for making their codes for numerical simulation publicly available.

Conflicts of Interest

Katsutoshi Murata is an employee of Siemens Healthcare K.K., Japan. Thorsten Feiweier is an employee of Siemens Healthcare GmbH, Germany. All remaining authors have no potential conflicts of interest associated with this work.

References

1. Tetsuka S. Reversible lesion in the splenium of the corpus callosum. Brain Behav 2019; 9:1–10.
2. Novikov DS, Fieremans E, Jespersen SN, Kiselev VG. Quantifying brain microstructure with diffusion MRI: Theory and parameter estimation. NMR Biomed 2019; 32:e3998.
3. Baron CA, Beaulieu C. Oscillating gradient spin-echo (OGSE) diffusion tensor imaging of the human brain. Magn Reson Med 2014; 72:726–736.
4. Fieremans E, Burcaw LM, Lee HH, Lemberskiy G, Veraart J, Novikov DS. In vivo observation and biophysical interpretation of time-dependent diffusion in human white matter. Neuroimage 2016; 129:414–427.
5. Baron CA, Kate M, Gioia L, et al. Reduction of diffusion-weighted imaging contrast of acute ischemic stroke at short diffusion times. Stroke 2015; 46:2136–2141.
6. Lemberskiy G, Rosenkrantz AB, Veraart J, Taneja SS, Novikov DS, Fieremans E. Time-dependent diffusion in prostate cancer. Invest Radiol 2017; 52:405–411.
7. Andica C, Hori M, Kamiya K, et al. Spatial restriction within intracranial epidermoid cysts observed using short diffusion-time diffusion-weighted imaging. Magn Reson Med Sci 2018; 17:269–272.
8. Harper PA, Healy PJ, Dennis JA. Maple syrup urine disease (branched chain ketoaciduria). Am J Pathol 1990; 136:1445–1447.
9. Fieremans E, Lee HH. Physical and numerical phantoms for the validation of brain microstructural MRI: a cookbook. Neuroimage 2018; 182:39–61.
10. Donev A, Torquato S, Stillinger FH. Neighbor list collision-driven molecular dynamics simulation for nonspherical hard particles. I. Algorithmic details. J Comput Phys 2005; 202:737–764.
11. Aboitiz F, Scheibel AB, Fisher RS, Zaidel E. Fiber composition of the human corpus callosum. Brain Res 1992; 598:143–153.
12. Harkins KD, Valentine WM, Gochberg DF, Does MD. *In-vivo* multi-exponential T2, magnetization transfer and quantitative histology in a rat model of intramyelinic edema. Neuroimage Clin 2013; 2:810–817.